Molecular self-assembly of surfactant-like peptides to form nanotubes and nanovesicles

Sylvain Vauthey*, Steve Santoso*†, Haiyan Gong*‡, Nicki Watson§, and Shuguang Zhang*¶

*Center for Biomedical Engineering, 56-341, Massachusetts Institute of Technology, 77 Massachusetts Avenue, Cambridge, MA 02139-4307; †Department of Biology, Massachusetts Institute of Technology, Cambridge, MA 02139; §W. M. Keck Imaging Facility, Whitehead Institute, Cambridge, MA 02142; and ‡Department of Ophthalmology, Boston University School of Medicine, 715 Albany Street, Boston, MA 02118

Communicated by John M. Buchanan, Massachusetts Institute of Technology, Cambridge, MA, February 13, 2002 (received for review November 17, 2001)

Several surfactant-like peptides undergo self-assembly to form nanotubes and nanovesicles having an average diameter of 30–50 nm with a helical twist. The peptide monomer contains 7–8 residues and has a hydrophilic head composed of aspartic acid and a tail of hydrophobic amino acids such as alanine, valine, or leucine. The length of each peptide is ≈2 nm, similar to that of biological phospholipids. Dynamic light-scattering studies showed structures with very discrete sizes. The distribution becomes broader over time, indicating a very dynamic process of assembly and disassembly. Visualization with transmission electron microscopy of quick-freeze/deep-etch sample preparation revealed a network of open-ended nanotubes and some vesicles, with the latter being able to "fuse" and "bud" out of the former. The structures showed some tail sequence preference. Many three-way junctions that may act as links between the nanotubes have been observed also. Studies of peptide surfactant molecules have significant implications in the design of nonlipid biological surfactants and the understanding of the complexity and dynamics of the self-assembly processes.

amino acids | charged and hydrophobic residues | nonlipid surfactants | simplicity to complexity | prebiotic enclosures

Molecular self-assembly recently has attracted considerable attention for its use in the design and fabrication of nanostructures leading to the development of advanced materials (1, 2). The self-assembly of biomolecular building blocks plays an increasingly important role in the discovery of new materials and scaffolds (3, 4), with a wide range of applications in nanotechnology and medical technologies such as regenerative medicine and drug delivery systems (5, 6). Recently, Hartgerink *et al.* (7) reported the design of a chimeric material consisting of a hydrophobic alkyl tail and a hydrophilic peptide containing phosphorylated serine with an RGD motif that facilitates directional alignment of mineralization of hydroxyapatite.

We previously described a class of ionic self-complementary peptide that spontaneously self-assemble to form interwoven nanofibers in the presence of monovalent cations (8–10). These nanofibers further form a hydrogel consisting of greater than 99.5% water. The constituent of the hydrogel scaffold is made of peptides with alternating hydrophilic and hydrophobic amino acids. Such a sequence has a tendency to form an unusually stable β-sheet structure in water (8–10). When the peptides form a β-sheet, they exhibit two surfaces, a hydrophilic surface consisting of charged ionic side chains and a hydrophobic surface with hydrophobic side chains. As a result, the self-assembly of these peptides is facilitated by electrostatic interactions on one side and the hydrophobic interaction on the other, in addition to the conventional β-sheet hydrogen bond along the backbones. The self-assembling peptide scaffolds have been demonstrated to serve as substrate for tissue-cell attachment, extensive neurite outgrowth, and formation of active nerve connections. Thus, the nanofiber hydrogel can be used as a permissive biological material for culturing cells in a three-dimensional environment (9).

In another attempt to exploit the intrinsic self-assembly of peptides as an avenue to emerging materials, Aggeli *et al.* (11, 12) have designed different short peptides that self-assemble in nonaqueous solvent into long, semiflexible, polymeric β-sheet peptide nanotapes. These systems were designed rationally to provide strong cross-strand-attractive forces between the side chains such as electrostatic, hydrophobic, or hydrogen-bonding interactions. In another study, Ghadiri and coworkers (13–15) produced self-assembling nanotubes made from alternating D,L-α-peptides and cyclic β-peptide. They first showed that D,L-peptides {cyclo-[-(L-Gln-D-Ala-L-Glu-D-Ala)$_2$-]} adopt flat, ring-shaped conformations and stack through backbone–backbone hydrogen bonding to form extended cylindrical structures with a diameter ≈1 nm in the single peptide tube. They further showed that this type of peptide nanotubes forms pores in the cell membrane (15).

We are interested in broadening the diversity of the building blocks of self-assembling peptides for scaffolds and biological materials. We therefore designed another class of amphiphilic surfactant-like peptides. These 7–8-residue peptides (Fig. 1), each ≈2 nm in length, have properties very similar to those observed in biological surfactant molecules. They have a hydrophilic head group of negatively charged aspartic acid at the C terminus, thus containing two negative charges (one from the side chain carboxyl group and the other from the C terminus) and a lipophilic tail made of hydrophobic amino acids such as alanine, valine, or leucine (Fig. 1). The N terminus is acetylated, making it uncharged. When dissolved in water, these surfactant-like peptides tend to self-assemble to isolate the hydrophobic tail from contact with water. Similar to lipids and fatty acids, the supramolecular structure is characterized by the formation of a polar interface that sequesters the hydrophobic tail from water.

Materials and Methods

Surfactant-Like Peptides. All peptides were synthesized with Wang resin and acetylated at their N termini. All were synthesized commercially (Synpep, Dublin, CA, or Research Genetics, Huntsville, AL) and solubilized in water to a concentration of ≈4–5 mM, and their pH values were neutralized with 0.1 N NaOH in small scintillation glass vials. The solutions were sonicated for 10 min in an Aquasonic Model 50HT water bath (VWR Scientific). All peptide solutions were stored and handled at room temperature.

Dynamic Light Scattering (DLS). An aliquot of 150–200 μl of the peptide solution was used to perform DLS experiments by using PDDLS/Batch (Precision Detectors, Franklin, MA). Intensity data from each sample were collected in five replicates and analyzed by using the PRECISION DECONVOLVE program and

Abbreviations: DLS, dynamic light-scattering; TEM, transmission electron microscopy.

¶To whom reprint requests should be addressed. E-mail: shuguang@mit.edu.

The publication costs of this article were defrayed in part by page charge payment. This article must therefore be hereby marked "*advertisement*" in accordance with 18 U.S.C. §1734 solely to indicate this fact.

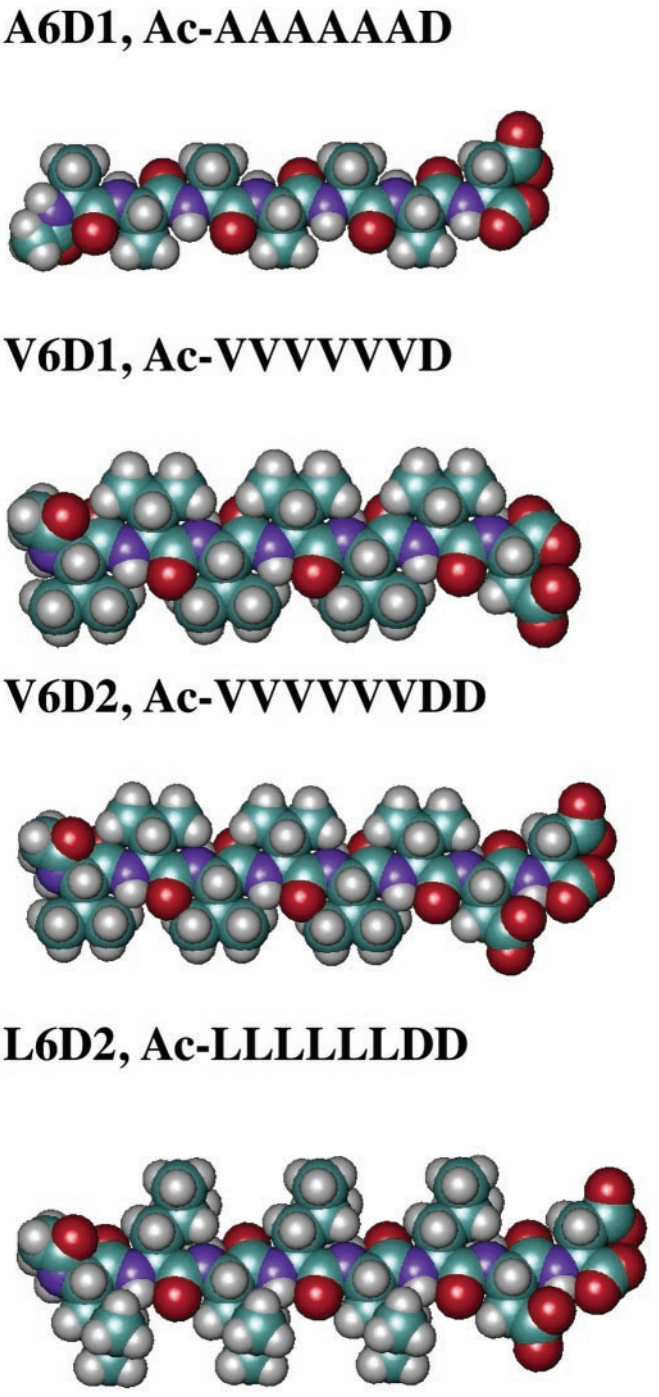

Fig. 1. Space-filling molecular models of surfactant peptide. (*A*) A_6D. (*B*) V_6D. (*C*) V_6D_2. (*D*) L_6D_2. D (aspartic acid) bears negative charges, and A (alanine), V (valine), and L (leucine) constitute the hydrophobic tails with increasing hydrophobicity. Green, carbons; red, oxygen; blue, nitrogen; white, hydrogen. Each peptide is ≈2–3 nm in length, similar to biological phospholipids.

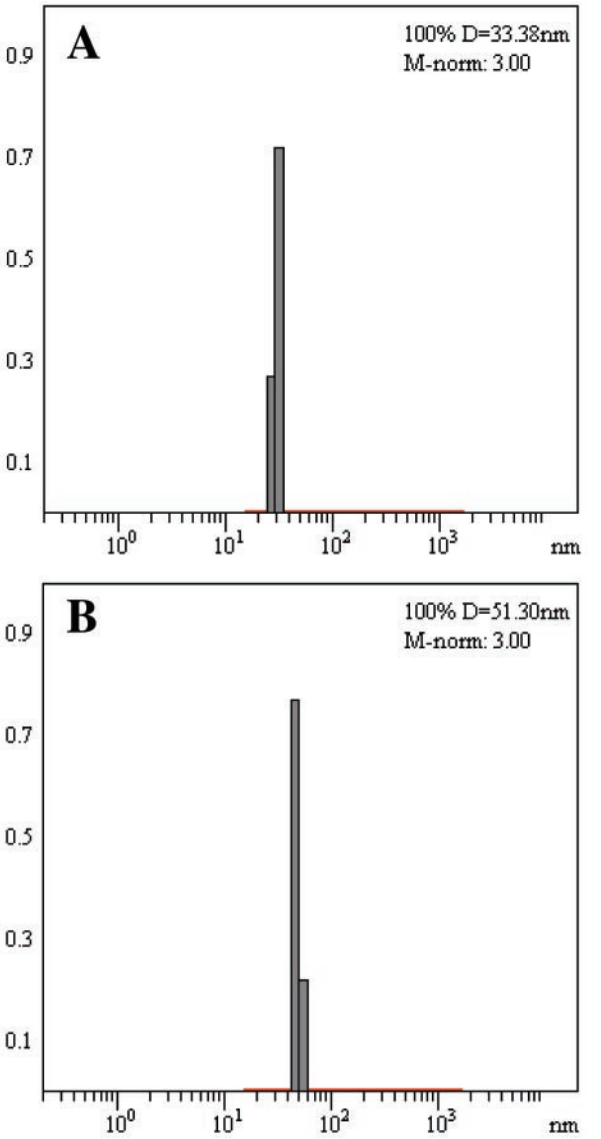

Fig. 2. DLS measurement of surfactant peptide nanostructures. The peptides V_6D, V_6D_2, and A_6D gave similar results. Intensity data were collected five times, each looking nearly identical to the rest. The *x* axis is the size in nanometers, and the *y* axis is the fraction distribution. The average diameter (D) is ≈30–50 nm. (*A*) A_6D. (*B*) V_6D. The other dimension along the length of the nanotube is beyond the range of DLS measurement.

yielded size-versus-fraction distribution plots. It was found that nanostructures formed in a narrow range of 30–50 nm (Fig. 2). DLS is a rapid screening method for defined nanostructures. Without discrete peak intensity, there are no nanostructures observed subsequently. These observations encouraged us to further study the structures by using a quick-freeze/deep-etch technique to preserve the structures as they appear in aqueous state and to examine them by using transmission electron microscopy (TEM).

Quick-Freeze/Deep-Etch Sample Preparation. Quick-freeze/deep-etch sample preparation for TEM followed the protocol described by Magid (16). Briefly, aliquots (1–2 μl) of peptides in water were placed on 3-mm gold specimen carriers. The samples then were frozen rapidly in liquid propane (−180 to −190°C) by using the TFD 010 plunge-freeze and transfer device (BALTEC, Balzers, Principality of Liechtenstein). The frozen samples were stored in liquid nitrogen and transferred onto a cold stage (−180°C) in the CFE-60 freeze fracture system (Cressington Scientific Instruments, Cranberry, PA). The sample holder was warmed to −100°C and the sample surface was etched for 30 min by placing a cooled knife (−180°C) directly above the samples. After etching, the specimens were rotary-shadowed with a 20° platinum-carbon gun. The estimated electron-dense coating thickness using this method was ≈1.5–2.0 nm as determined by a quartz crystal thin-film monitor. Replicas were strengthened by evaporation of carbon at an angle of 90°. The thickness of the

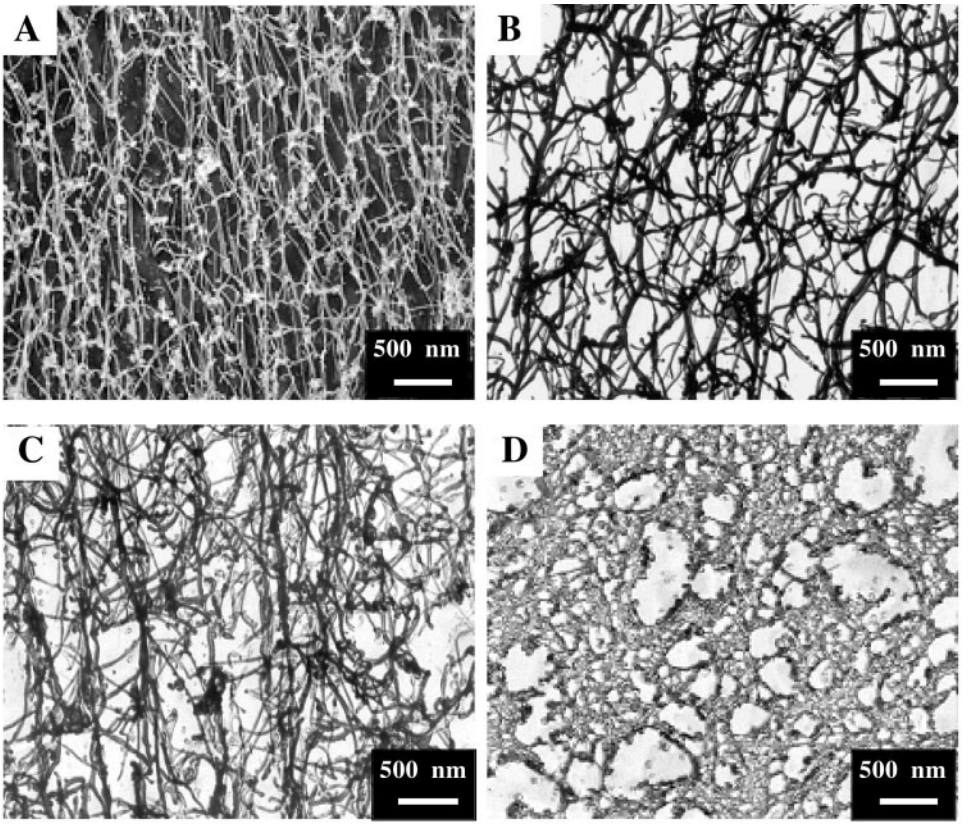

Fig. 3. Quick-freeze/deep-etch TEM image of the surfactant peptides A_6D, V_6D, V_6D_2, and L_6D_2 in water (4.3 mM). These peptides self-assembled into a dense network extended to several micrometers in length. Because the droplet solution containing the peptide nanotubes is in three dimensions, the network of a two-dimensional image appears denser than the actual structure, similar to looking at a picture of the branches on a tree without leaves. (*A*) A_6D. (*B*) V_6D. (*C*) V_6D_2. (*D*) L_6D_2.

carbon surface was ≈15–20 nm. After shadowing, the sample with the replica coating was stored in methanol overnight and then treated in 5% sodium hypochloride containing 10–15% potassium hydroxide or bleach to degrade the peptides. The remaining replicas were washed several times in distilled water and floated onto copper Gilder grids (Electron Microscopy Sciences, Fort Washington, PA). The replicas were examined by using a Philips-300 or Philips EM-410 TEM (Philips, Eindhoven, the Netherlands).

Results and Discussion

Design of Surfactant Peptides. The sequences and molecular models of several surfactant peptides are shown in Fig. 1. The hydrophilic moiety of the molecule is provided by 1–2 aspartic acids at the C termini such that the peptide would have two or three negative charges, similar to biological phospholipids. The hydrophobic tails of the peptides consist of six consecutive hydrophobic amino acids with an acetylated N terminus, eliminating the positive charge. The lengths and overall hydrophobicity of these peptides can be fine-tuned by modifying the aliphatic side groups of the amino acids. The calculated pI for the investigated peptides range from 3.56 to 3.8 depending on the number of aspartic acids constituting the polar head group. At neutral pH, the aspartic acids are negatively charged, but when the pH of the peptide solutions is below 3.5, the aspartic acids become protonated, the peptides are uncharged, and their solubility in water becomes compromised substantially.

The hydrophobic tails of the peptides contain alanine (A), valine (V), or leucine (L) with increasing size of the hydrocarbon side chain and thus hydrophobicity. Various residues have influence in the intermolecular interactions and packing of the tails. In the surfactant peptides, V_6D_2 and L_6D_2, the hydrophilic heads have a common aspartic acid, whereas the tails varied in hydrophobicity (Fig. 1). After self-assembly, these peptides may form different structures with different physical parameters, because packing of the hydrophobic side chains depends on the sizes of their corresponding van der Waals surface areas. Likewise, by looking at both V_6D and V_6D_2 we tested whether the addition of one aspartic acid to the head group would make a difference in the size and/or shape of the aggregates formed. This phenomenon is well described in the surfactant field as the packing parameter by Israelachvili *et al.* (17) [$P = v/(a \cdot l)$], where P is the packing parameter, v is the molecular volume, l is the molecular length, and a is the cross-sectional area of the polar head group. It should be noted that A_6D and V_6D carry two negative charges at the C termini, and A_6D_2, A_6D, V_6D_2, and L_6D_2 consist of three negative charge groups. A simple modification of the peptide sequence will result in the change of the charge ratio with a significant impact in its solubility. If there is too much charge, they become too soluble and may repel each other electrostatically. On the other hand, if there are too many hydrophobic residues, the peptides will become insoluble in water. A_6D, V_6D, and V_6D_2 showed similar nanostructures but with varied sizes. However, peptide L_6D_2 exhibited a quite different structure, suggesting that the hydrophobic tail packing is different, probably because of leucine large side chains (Figs. 1*D* and 3*D*).

Size of Nanostructures Studied Using DLS. To quickly assess the formation of supramolecular structures through self-assembly,

we performed DLS experiments. The observation of a monodisperse population with sizes in the range of 30–50 nm for A_6D, V_6D, and V_6D_2 suggested the formation of regular structure(s) from the peptide building blocks (Fig. 2 *A* and *B*, not shown for V_6D_2). As indicated above, we expected the packing parameters of these peptides to affect the shape and size of the assemblies that they formed significantly. In this study, the polar head group did not significantly influence the size of the nanostructures, suggesting that either more aspartic acids or a charged amino acid with a longer carboxylic acid tether is needed. Interestingly, the distribution of structures became more polydisperse over time (data not shown), implying the process in which these peptides interact with each other is very dynamic. The polydisperse samples also did not produce regular nanostructures when examined by using the quick-freeze/deep-etch method under TEM.

TEM Examination of Samples Prepared Through the Quick-Freeze/Deep-Etch Procedure. The quick-freeze/deep-etch sample preparation procedure has minimal disturbance of the structures formed in solution. TEM images revealed that the surfactant peptides formed a dense network of nanotubes and nanovesicles, with diameters ranging from 30 to 50 nm (Figs. 3 and 4), which is consistent with the measurement from DLS. The peptide assemblies represent a three-dimensional network similar to flexible polymers in their semidilute or concentrated solutions (18). It should be pointed out that under the TEM, only a two-dimensional projection of the specimen could be imaged. The network below and above the focal point in the space could be relatively distant in three dimensions while appearing superimposed in the two-dimensional projection, thus appearing denser than it actually is. This is similar to looking at a picture of the branches on a tree without leaves; the network seems denser on a two-dimensional photo than on the actual object. TEM images of A_6D, V_6D, and V_6D_2 exhibit very similar tubular morphologies. These self-assemblies have high axial ratios and can extend in length to tens of micrometers (Fig. 3). Furthermore, 3-fold junctions or branches connecting the nanotubes forming the network can be identified, similar to those observed in tree branches (Fig. 4).

The possibility of branched supramolecular organizations has attracted considerable interest (19–21). Evidence of branching has been reported mainly for aqueous surfactant solutions, but reversed structure such as lecithin organogels also can form three-way junctions (22). Branch points produce patches having a mean curvature opposite to that of the portion far from the junction (22). Many reports claimed the importance of branching points in the visco-elastic properties of polymer-like systems. Cates (21, 22) provided a statistical description of branches versus entanglements and Lequeux (23) modeled the expected effects on the rheological properties.

TEM images show a dense network of nanotubes ≈30–50 nm in diameter linked by a number of 3-fold junctions. L_6D_2 is the most hydrophobic molecule, with a tail containing six leucines. Aqueous solution of L_6D_2 exhibits a heterogeneous population of nanotubes and entangled rod-like micelles and vesicles (Fig. 3*D*). These molecular assemblies are similar to string-like micellar systems made from traditional amphiphilic molecules such as cetyltrimethylammonium bromide (CTAB; refs. 24 and 25). In this case, DLS did not provide detailed insight into the size of any regular structures formed and perhaps only captured the average size of the entanglements.

TEM images at high magnification provide a detailed structure of the peptide nanotubes for the other three peptides (Fig. 4). The presence of hollow tubules for A_6D is clearly visible (Fig. 4*A*, red arrows), giving rise to two spatially separated hydrophilic surfaces. Additionally, right-handed helical twists with 150–200-nm pitches depending on the nanotube diameters also were

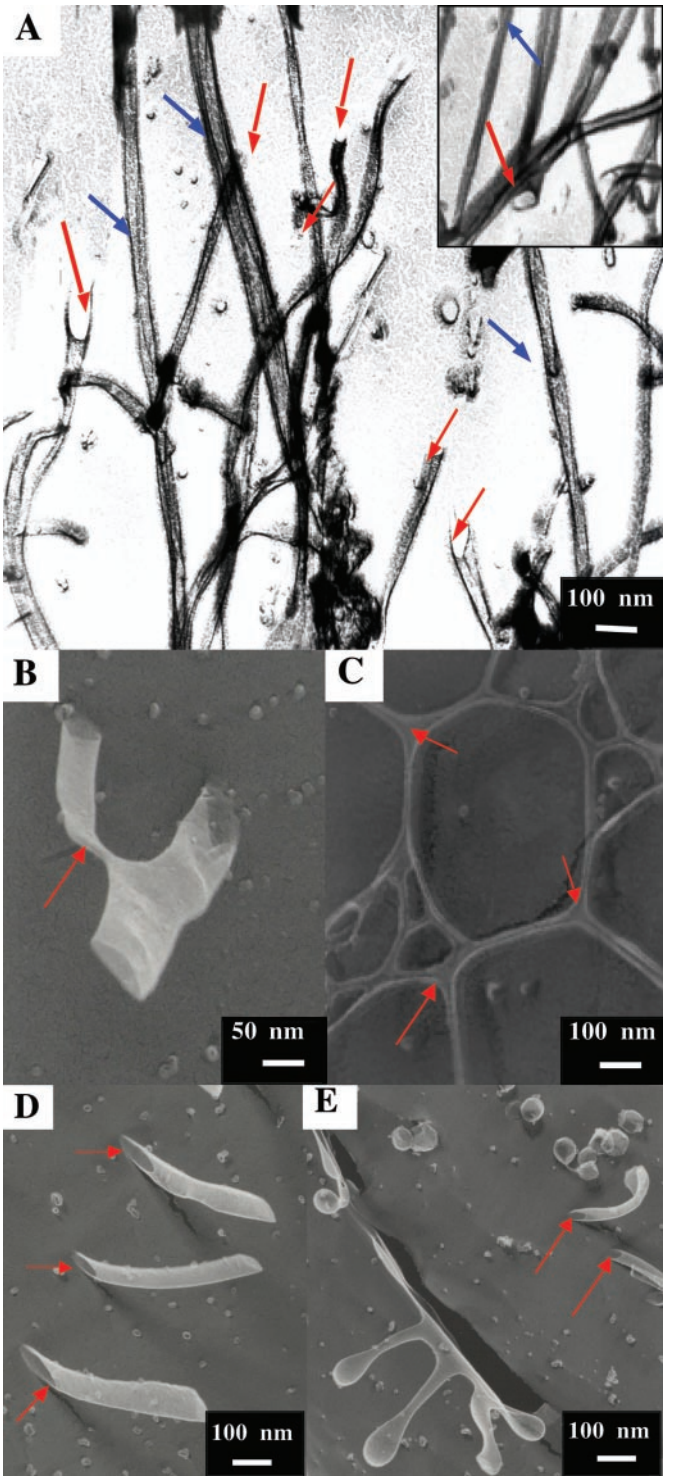

Fig. 4. (*A*) Quick-freeze/deep-etch TEM image of A_6D and V_6D dissolved in water (4.3 mM at pH 7) at high-resolution. The images show the dimensions, 30–50 nm in diameter with openings of nanotube ends (red arrows). (*Inset*) Opening ends in more detail. Note some opening ends of the peptide nanotube may be cut vertically. The strong contrast shadow of the platinum coat also suggests the hollow tubular structure. Similar lipid right-handed helical tubular nano- and microstructures have been reported (26, 27). *B* and *C* show a three-way junction and many three-way junctions, respectively. There are openings at the ends (*D* and *E*, indicated by red arrows), with the other ends possibly buried inside the replica. There also are some vesicles and nanotubes in the upper right corner (*E*, arrows point to the hollow opening at the ends). Micelles and vesicles are present also. (*E*) Example of vesicles that are budding off of a nanotube.

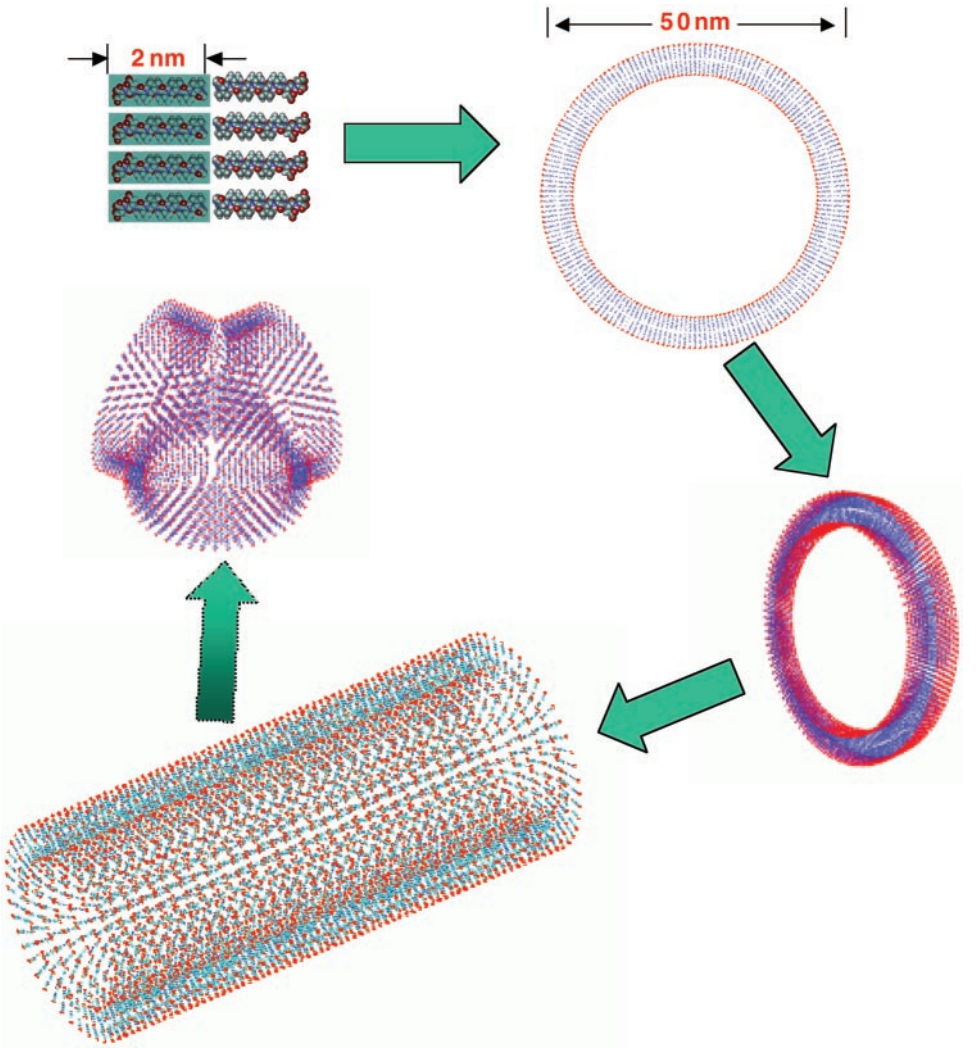

Fig. 5. Potential pathway of V_6D peptide nanotube formation. Each peptide monomer is 2 nm, and the diameter of the modeled bilayer nanotube is 50 nm. Red, hydrophilic head; blue, hydrophobic tail. Each peptide may interact with one another to form closed rings, which in turn stack on top of one another, ultimately yielding a nanotube. Three nanotubes are connected to each other through a three-way junction. This phenomenon mirrors lipid microtubule structures (26, 27).

observed (Fig. 4*A*, blue arrows). Open-ended tubes and a three-way junction also are shown in high magnification (Fig. 4 *B* and *C*). Interestingly, we also observed plausible budding or fusion of nanovesicles from the V_6D nanotube (Fig. 4*D*), suggesting the dynamic behavior of the self-assembly process of these surfactant peptides.

Other Structural Aspects. Circular dichroism studies revealed a single minimum spectrum at 220 nm that does not resemble either β-sheet or α-helical structure (data not shown). This observation may reflect an unusual chirality of the assembled structures that do not have typical β-sheet packing. Spector *et al.* (26) also used circular dichroism to study the chirality of diacetylenic lipid tubules formed from lipid bilayer membranes. Schnur and coworkers (26, 27) developed a theory based on molecular chirality to explain the presence of helical markings on the twist of lipid tubules.

It should be pointed out that the light-scattering experiments suggest that self-assembly is a dynamic process, and the size distributions are not static over long periods. Although it seems that the structures of A_6D and V_6D are rather similar except the initial diameter size, they also change over time from constant assembly and disassembly.

Molecular Modeling. How could these simple surfactant-like peptides form such well ordered nanotubes and nanovesicles? There are molecular and chemical similarities between lipids and the peptides, because both have a hydrophilic head and a hydrophobic tail. The packing between lipids and peptides are likely to be quite different, however. In lipids, the hydrophobic tails pack tightly against each other to completely displace water, precluding the formation of hydrogen bonds. On the other hand, in addition to hydrophobic tail packing between the amino acid side chains, surfactant peptides also may interact through intermolecular hydrogen bonds along the backbone. To understand how each peptide molecule interacts with one another, we modeled the nanotube from the constituent building block. It should be noted that a complete molecular simulation of the self-assembly process is beyond our current computational capability.

We propose the simplest structure of a peptide nanotube through molecular modeling of V_6D (Fig. 5) and a possible path

from the monomer state to the assemblies. Each peptide monomer is 2 nm, with the diameter of the observed tube being 50 nm. Two peptides form dimeric tail-to-tail packing to form a bilayer creating a unilamellar shell with a maximum thickness of 4 nm. Had they formed a multilamellar structure, the opening ends may not have exhibited a clearly observed single-shell ring structure when viewed with the TEM. Furthermore, the strong contrast shadow of the platinum coat also suggested that the tubes are hollow, similar to the lipid microtubes. These surfactant peptides may form tubular structures akin to those found in lipid systems (27). Individual peptides are intrinsically twisted such that assembled structures will likely have a curvature. One of the simplest pathways of formation may be that the monomeric peptides form small segments of the bilayer ring, with hydrophobic tails packing together to avoid water and hydrophilic heads exposed to water on the inner and outer portion of the tube. Through continuous dynamic energy minimization, they grow into single subunit rings and multirings, in which aspartic acid hydrophilic groups remain exposed to the continuous aqueous medium. The tubular arrays may subsequently stack through noncovalent interactions to form longer nanotubes. This proposed model remains to be clarified experimentally and computationally.

Synthetic Peptide Surfactant. Although there are several types of nanotubes ranging from carbon, D,L-cyclical peptides (13–15), and lipids (26, 27), our system is complementary to them. The surfactant peptides are relatively inexpensive and chemically facile to modify, leading to potential tailoring of new materials for a broad spectrum of applications, including serving as scaffolds to organize conducting and semiconducting nanocrystals into high-density ordered structures; incorporating other biomolecules on their surfaces; encapsulating molecules for molecular deliveries; and forming a scaffold for cell encapsulation. Moreover, the molecular self-assembly process of surfactant peptide mirrors the lipid-surfactant assemblies. Thus a wealth of literature and methods can be used as a guide for further studies.

Peptides in general have not been considered seriously to be useful materials as scaffolds because of their small size and less defined structures at the individual monomeric level. However, several self-assembling peptide systems have not only introduced designed peptides as molecular building blocks but also may inspire others to uncover and develop additional self-assembling systems. Nanotubes and nanovesicles from self-assembly of this class of surfactant-like peptides are one of the simplest systems that can lead to formation of the well defined complex structures. The phenomena from simplicity to complexity also occur in other natural self-assembly systems including nucleic acids, lipids, saccharides, and proteins. It is anticipated that self-assemblies and fine-tuning of the surfactant peptide building blocks will lead to construction of a wide range of nanostructures, fostering innovative avenues for the development of scaffold and biologically inspired materials.

This surfactant peptide system also may capture the prebiotic environment's simple origin and complex outcome. It is possible to study molecular reorganizations, replications, and evolution in a simple enclosed environment of a peptide nanovesicle and a closed-ended nanotube.

We thank Geoffrey von Maltzahn for sharing unpublished results and Wonmuk Hwang and Davide Marini for molecular modeling of the surfactant peptide nanotubes. We also thank Alexander Rich, Carlos Semino, Joseph Jacobson, Hyman Hartman, Jianping Shi, Kim Hamad, Shuwang An, Mark Spector, Joel Schnur, and Daniel Blankschtein for stimulating and helpful discussions. This work is supported in part by grants from the U.S. Army Research Office, Naval Research Labs/Defense Advanced Research Project Agency, and National Institutes of Health. We also thank Intel Corporation for educational donation of high-speed computers for molecular modeling.

1. Whitesides, G. M., Mathias, J. P. & Seto, C. T. (1991) *Science* **254,** 1312–1319.
2. Lehn, J. M. (1993) *Science* **260,** 1762–1763.
3. Alivisatos, A. P., Johnsson, K. P., Peng, X., Wilson, T. E., Loweth, C. J., Bruchez, M. P., Jr. & Schultz, P. G. (1996) *Nature* (*London*) **382,** 609–611.
4. Mirkin, C. A., Letsinger, R. L., Mucic, R. C. & Storhoff, J. J. (1996) *Nature* (*London*) **382,** 607–609.
5. Langer, R. S. & Vacanti, J. P. (1993) *Science* **260,** 920–926.
6. Hubbell, J. A. (1999) *Curr. Opin. Biotechnol.* **10,** 123–129.
7. Hartgerink, J. D., Beniash, E. & Stupp, S. I. (2001) *Science* **294,** 1684–1688.
8. Zhang, S., Holmes, T., Lockshin, C. & Rich, A. (1993) *Proc. Natl. Acad. Sci. USA* **91,** 1345–1349.
9. Holmes, T. C., De Lecalle, S., Su, X., Liu, G., Rich, A. & Zhang, S. (2000) *Proc. Natl. Acad. Sci. USA* **97,** 6728–6733.
10. Caplan, M., Moore, P., Zhang, S., Kamm, R. D. & Lauffenburger, D. A. (2001) *Biomacromolecules* **4,** 627–631.
11. Aggeli, A., Bell, M., Boden, N., Keen, J. N., Knowles, P. F., McLeish, T. C. B., Pitkeathly, M. & Radford, S. E. (1997) *Nature* (*London*) **386,** 259–262.
12. Aggeli, A., Nyrkova, I. A., Bell, M., Harding, R., Carrick, L., McLeish, T. C. B., Semenov, A. N. & Boden, N. (2001) *Proc. Natl. Acad. Sci. USA* **98,** 11857–11862.
13. Ghadiri, M. R., Granja, J. R. & Buehler, L. K. (1994) *Nature* (*London*) **369,** 301–304.
14. Bong, D. T., Clark, T. D., Granja, J. R. & Ghadiri, M. R. (2001) *Angew. Chem. Int. Ed. Engl.* **40,** 988–1011.
15. Fernandez-Lopez, S., Kim, H. S., Choi, E. C., Delgado, M., Granja, J. R., Khasanov, A., Kraehenbuehl, K., Long, G., Weinberger, D. A., Wilcoxen, K. M. & Ghadiri, M. R. (2001) *Nature* (*London*) **41,** 452–455.
16. Magid, J. L. (1998) *J. Phys. Chem. B* **102,** 4064–4074.
17. Israelachvili, J. N., Mitchell, D. J. & Ninham, B. W. (1976) *J. Chem. Soc. Faraday Trans. 2* **72,** 1525–1568.
18. Shchipunov, Y. A. & Hoffmann, H. (1998) *Langmuir* **14,** 6350–6360.
19. Drye, T. J. & Cates, M. E. J. (1993) *J. Chem. Phys.* **98,** 9790–9797.
20. Shikata, T. & Imai, S. (2000) *Langmuir* **16,** 4840–4845.
21. Cates, M. E. (1987) *Macromolecules* **20,** 2289–2296.
22. Cates, M. E. (1988) *J. Phys.* **49,** 1593–1600.
23. Lequeux, F. (1996) *Curr. Opin. Colloid Interface Sci.* **1,** 341–344.
24. Nemoto, N., Kuwahara, M., Yao, M. L. & Osaki, K. (1995) *Langmuir* **11,** 30–36.
25. Hassan, P. A. & Yakhmi, J. V. (2000) *Langmuir* **16,** 7187–7191.
26. Spector, M. S., Easwaran, K. R., Jyothi, G., Selinger, J. V., Singh, A. & Schnur, J. M. (1996) *Proc. Natl. Acad. Sci. USA* **93,** 12943–12946.
27. Selinger, J. V., MacKintosh, F. C. & Schnur, J. M. (1996) *Phys. Rev. E Stat. Phys. Plasmas Fluids Relat. Interdiscip. Top.* **53,** 3804–3818.